

PARTICLE CONFIGURATIONS AND COXETER OPERADS

SUZANNE M. ARMSTRONG, MICHAEL CARR, SATYAN L. DEVADOSS, ERIC ENGLER,
ANANDA LEININGER, AND MICHAEL MANAPAT

ABSTRACT. There exist natural generalizations of the real moduli space of Riemann spheres based on manipulations of Coxeter complexes. These novel spaces inherit a tiling by the graph-associahedra convex polytopes. We obtain explicit configuration space models for the classical infinite families of finite and affine Weyl groups using particles on lines and circles. A Fulton-MacPherson compactification of these spaces is described and this is used to define the Coxeter operad. A complete classification of the building sets of these complexes is also given, along with a computation of their Euler characteristics.

1. MOTIVATION FROM PHYSICS

1.1. A configuration space of n ordered, distinct particles on a variety V is

$$C_n(V) = V^n - \Delta, \quad \text{where } \Delta = \{(x_1, \dots, x_n) \in V^n \mid \exists i, j, x_i = x_j\}.$$

Over the past decade, there has been an increased interest in the configuration space of n labeled particles on the projective line. The focus is on a quotient of this space by $\mathbb{P}\mathrm{GL}_2(\mathbb{C})$, the affine automorphisms on $\mathbb{C}\mathbb{P}^1$. The resulting variety is the moduli space of Riemann spheres with n punctures $\mathcal{M}_{0,n} = C_n(\mathbb{C}\mathbb{P}^1)/\mathbb{P}\mathrm{GL}_2(\mathbb{C})$. There is a compactification $\overline{\mathcal{M}}_{0,n}$ of this space, a smooth variety of complex dimension $n-3$, coming from Geometric Invariant Theory [24]. The space $\overline{\mathcal{M}}_{0,n}$ plays a crucial role as a fundamental building block in the theory of Gromov-Witten invariants, also appearing in symplectic geometry and quantum cohomology [20].

Our work is motivated by the *real* points $\overline{\mathcal{M}}_{0,n}(\mathbb{R})$ of this space, the set of points fixed under complex conjugation. These real moduli spaces have importance in their own right, appearing in areas such as ζ -motives of Goncharov and Manin [17] and Lagrangian Floer theory of Fukaya [15]. Indeed, $\overline{\mathcal{M}}_{0,n}(\mathbb{R})$ has even emerged in phylogenetic trees [2] and networks [21]. It was Kapranov [19] who first noticed a relationship between $\overline{\mathcal{M}}_{0,n}(\mathbb{R})$ and the braid arrangement of hyperplanes, associated to the Coxeter group of type A : Blow-ups of certain cells of the A_n Coxeter complex yield a space homeomorphic to a double cover of $\overline{\mathcal{M}}_{0,n+2}(\mathbb{R})$. This creates a natural tiling of $\overline{\mathcal{M}}_{0,n}(\mathbb{R})$ by associahedra, the combinatorics of which is discussed in [12]. Davis et. al have generalized this construction to all Coxeter groups, along with studying the fundamental groups of these blow-up spaces [8]. Carr and Devadoss [6] looked at the inherent tiling of these spaces by the convex polytopes *graph-associahedra*.

2000 *Mathematics Subject Classification*. Primary 18D50, Secondary 14H10, 52B11.

All authors were partially supported by NSF grant DMS-9820570. Carr and Devadoss were also supported by NSF CARGO grant DMS-0310354.

1.2. We begin with elementary results and notation: Section 2 provides the background of Coxeter groups and their associated Coxeter complexes and Section 3 constructs the appropriate configuration spaces of particles. Section 4 introduces the bracketing notation in order to visualize collisions in the configuration spaces, leading to viewing the hyperplanes of the Coxeter complexes in this new language. It is this notation that provides a transparent understanding of several results in this paper. In particular, it allows for a complete classification of the minimal building sets for the Coxeter complexes, along with their enumeration, as given in Tables 3 and 4. It is interesting to note that some configuration structures behave quite classically, whereas others (based on *thick* particles) are atypical.

The heart of the paper begins in Section 5 where the Fulton-MacPherson compactification [16] of these spaces is discussed and used to define the notion of a *Coxeter operad* in Definition 5.8, extending the mosaic operad of $\overline{\mathcal{M}}_{0,n}(\mathbb{R})$ [10]. Here, *nested* bracketings are used to describe the structure of the compactified spaces, enabling us to describe how the chambers of these spaces glue together. Section 6 ends with combinatorial results using the theory developed in [6]. For instance, the Euler characteristics of these Coxeter moduli spaces are given, exploiting the tilings by graph-associahedra.

As of writing this paper, the importance of the operadic structure of $\overline{\mathcal{M}}_{0,n}(\mathbb{R})$ has been brought further to light. For instance, Etingof et al. [13] have used the mosaic operad to compute the cohomology ring of $\overline{\mathcal{M}}_{0,n}(\mathbb{R})$. Recently, the Coxeter operad defined below appears in the work of E. Rains in computing the integral homology of these generalized Coxeter moduli spaces [28].

Acknowledgments. We express our gratitude to Jim Stasheff and Vic Reiner for detailed comments on this work and to Alex Postnikov for working on the f -vectors of graph-associahedra. We also thank the referee for wonderful insight and careful analysis, especially with regards to the operad module structures.

2. SPHERICAL AND EUCLIDEAN COMPLEXES

2.1. In order to provide the construction of Coxeter moduli space generalizations of $\overline{\mathcal{M}}_{0,n}(\mathbb{R})$, as given in Section 5, we begin with standard facts and definitions about Coxeter systems. Most of the material here can be found in Bourbaki [4].

Definition 2.1. Given a finite set S , a *Coxeter group* W is given by the presentation

$$W = \langle s_i \in S \mid s_i^2 = 1, (s_i s_j)^{m_{ij}} = 1 \rangle,$$

where $m_{ij} = m_{ji}$ and $2 \leq m_{ij} \leq \infty$. The pair (W, S) is called a *Coxeter system*.

Associated to any Coxeter system (W, S) is its *Coxeter graph* Γ_W : Each node represents an element of S , where two nodes s_i, s_j determine an edge if and only if $m_{ij} \geq 3$. A Coxeter group is *irreducible* if its Coxeter graph is connected and it is *locally finite* if either W is finite or each proper subset of S generates a finite group. A Coxeter group is *simplicial* if it is irreducible and locally finite [8]. The classification of simplicial Coxeter groups and their graphs is well-known [4, Chapter 6].

We restrict our attention to infinite families of simplicial Coxeter groups which generalize to arbitrary number of generators. This will mimic configuration spaces of an arbitrary number of

particles since our motivation comes from $\overline{\mathcal{M}}_{0,n}(\mathbb{R})$; it will also allow a well-defined construction of an operad. There are only seven such types of Coxeter groups: three spherical ones and four Euclidean ones. Figure 1 shows the Coxeter graphs associated to the Coxeter groups of interest; we label the edge with its order for $m_{ij} > 3$. The number of nodes of a graph is given by the subscript n for the spherical groups, whereas the number of nodes is $n + 1$ for the Euclidean case.

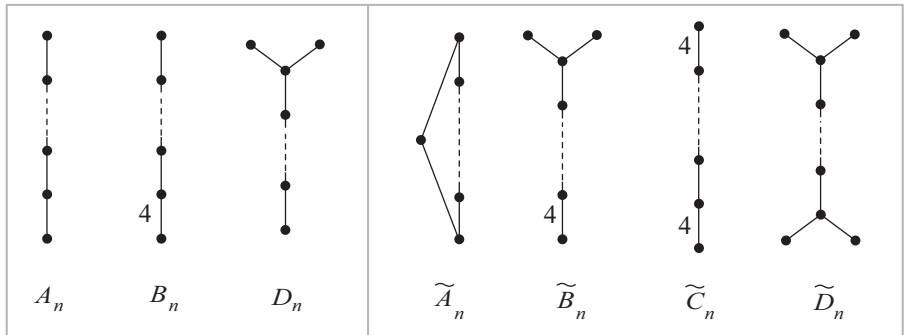


FIGURE 1. Coxeter graphs of spherical and Euclidean groups.

2.2. Every spherical Coxeter group has an associated finite reflection group realized by reflections across linear hyperplanes on a sphere. Every conjugate of a generator s_i acts on the sphere as a reflection in some hyperplane, dividing the sphere into simplicial chambers. The sphere, along with its cellulation is the *Coxeter complex* corresponding to W , denoted CW . The hyperplanes associated to each group given in Table 1 lie on the $(n - 1)$ sphere. The W -action on the chambers of CW is simply transitive, and thus we may associate an element of W to each chamber. The number of chambers of CW comes from the order of the group.

W	Hyperplanes	# Chambers
A_n	$x_i = x_j$	$(n + 1)!$
B_n	$x_i = 0, x_i = \pm x_j$	$2^n n!$
D_n	$x_i = \pm x_j$	$2^{n-1} n!$

TABLE 1. The spherical arrangements.

We move from spherical geometry coming from linear hyperplanes to Euclidean geometry arising from affine hyperplanes. Just as with the spherical case, each Euclidean Coxeter group has an associated Euclidean reflection group realized as reflections across affine hyperplanes in Euclidean space. Again, we focus on the infinite families of such Euclidean Coxeter groups which are $\tilde{A}_n, \tilde{B}_n, \tilde{C}_n,$ and \tilde{D}_n . The hyperplanes associated to each group, given in Table 2, lie in \mathbb{R}^n .

We look at the quotient of the Euclidean space \mathbb{R}^n by a group of translations, resulting in the n -torus \mathbb{T}^n . This is done for three reasons: First, the configuration space model is a more natural object after the quotient, resulting in particles on circles. Second, it is the correct generalization of

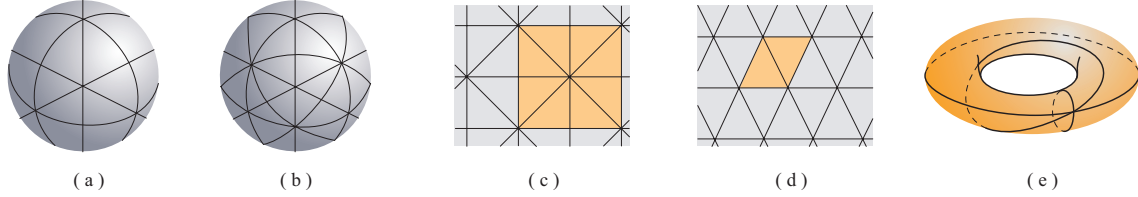
W	Hyperplanes ($k \in 2\mathbb{Z}$)	# Chambers
\tilde{A}_n	$x_i = x_j + k$	$n!$
\tilde{B}_n	$x_i = \pm x_j + k, x_i = 1 + k$	$2^{n-1} n!$
\tilde{C}_n	$x_i = \pm x_j + k, x_i = 1 + k, x_i = 0 + k$	$2^n n!$
\tilde{D}_n	$x_i = \pm x_j + k$	$2^{n-2} n!$

TABLE 2. The toroidal arrangements.

the affine type A complex, as discussed in [11]. Third, and most importantly, it presents us with valid operad module structures as given in Section 5.

The translations for \tilde{A}_n are covered in [11, Section 2.3]. For the remaining cases, we choose a slightly non-standard collection of hyperplanes in order for the associated configuration spaces to be more canonical. This has the benefit of identifying the most ubiquitous set of hyperplanes $\{x_i = \pm x_j + k\}$, producing an arrangement that is familiar from the spherical cases. We refer to the quotient of the complex CW of Euclidean type as the *toroidal Coxeter complex*, denoted \mathbb{TCW} .

Example 2.2. Figure 2(a) is \mathcal{CA}_3 , the 2-sphere with hyperplane markings, and part (b) is the 2-sphere \mathcal{CB}_3 . Figure 2(c) shows the hyperplanes of $\tilde{\mathcal{C}}_2$ in \mathbb{R}^2 , whereas (d) shows the hyperplanes for $\tilde{\mathcal{A}}_2$. Part (e) is the cellulation of the toroidal complex $\mathbb{TC}\tilde{\mathcal{A}}_2$.

FIGURE 2. Coxeter complexes (a) \mathcal{CA}_3 , (b) \mathcal{CB}_3 , (c) $\tilde{\mathcal{C}}_2$, (d) $\tilde{\mathcal{A}}_2$ and (e) $\mathbb{TC}\tilde{\mathcal{A}}_2$.

3. CONFIGURATION SPACES

3.1. We now give an explicit configuration space analog to each Coxeter complex above. These appear as (quotients of) configuration spaces of particles on the line \mathbb{R} and the circle \mathbb{S} . The arguments used for the constructions below are elementary, immediately following from the hyperplane arrangements of the reflection groups. However, as shown in Section 5, the configuration space model we provide will enable us to elegantly capture the blow-ups of these Coxeter complexes.

Definition 3.1. Let $C_n(\mathbb{R}) = \mathbb{R}^n - \{(x_1, x_2, \dots, x_n) \in \mathbb{R}^n \mid \exists i, j, x_i = x_j\}$ be the configuration space of n labeled particles on the real line \mathbb{R} . A generic point in $C_5(\mathbb{R})$ is $x_1 < x_2 < x_3 < x_4 < x_5$, which we notate (without labels) as $\circ - \circ - \circ - \circ - \circ$.

Definition 3.2. Let $C_{\bar{n}}(\mathbb{R}_{\bullet}) = \mathbb{R}^n - \{(x_1, x_2, \dots, x_n) \in \mathbb{R}^n \mid \exists i, j, x_i = \pm x_j \text{ or } x_i = 0\}$ be the space of n pairs of *symmetric* labeled particles (denoted \bar{n}) across the origin. A point in $C_3(\mathbb{R}_{\bullet})$

is $-x_3 < -x_2 < -x_1 < 0 < x_1 < x_2 < x_3$, which is depicted without labels as $\circ-\circ-\circ-\bullet-\circ-\circ-\circ$, where the black particle is fixed at the origin.

Definition 3.3. Let $C_{\bar{n}}(\mathbb{R}_o) = \mathbb{R}^n - \{(x_1, x_2, \dots, x_n) \in \mathbb{R}^n \mid \exists i, j, x_i = \pm x_j\}$ be the space of \bar{n} pairs of symmetric labeled particles across the origin, where the particle x_i and its symmetric partner $-x_i$ are both allowed to occupy the origin. A point in $C_{\bar{3}}(\mathbb{R}_o)$ is

$$(3.1) \quad -x_3 < -x_2 < -x_1, x_1 < x_2 < x_3$$

drawn $\circ-\circ-\circ-\circ-\circ-\circ-\circ$ without labels. Notice the mark at the origin where there is no fixed particle: The point $-x_3 < -x_2 < x_1, -x_1 < x_2 < x_3$ drawn as $\circ-\circ-\circ-\circ-\circ-\circ-\circ$ lies in the same chamber of $C_{\bar{3}}(\mathbb{R}_o)$ as Eq.(3.1).

Let $\text{Aff}(\mathbb{R})$ be the group of affine transformations of \mathbb{R} generated by translating and positive scaling. The action of $\text{Aff}(\mathbb{R})$ on $C_n(\mathbb{R})$ translates the leftmost of the n particles in \mathbb{R} to -1 and the rightmost is scaled to 1. If we allow the particles in $C_n(\mathbb{R})/\text{Aff}(\mathbb{R})$ to *collide* (coincide with each other), the resulting space is denoted $C_n\langle\mathbb{R}\rangle$. In a sense, this includes the hyperplanes which were removed back into \mathbb{R}^n . The space $C_n\langle\mathbb{R}\rangle$ is sometimes referred to as the *naive compactification* of $C_n(\mathbb{R})/\text{Aff}(\mathbb{R})$.¹

Proposition 3.4. $C_n\langle\mathbb{R}\rangle$ has the same cellulation as \mathcal{CA}_{n-1} .

A detailed proof of this is given in [12, Section 4]. Roughly, quotienting by translations of $\text{Aff}(\mathbb{R})$ removes the inessential component of the arrangement and scaling results in restricting to the sphere \mathcal{CA}_{n-1} . This proposition can be extended to the other spherical Coxeter complexes. Let $\text{Aff}(\bar{\mathbb{R}})$ be the transformations of \mathbb{R} generated simply by positive scalings: The action of $\text{Aff}(\bar{\mathbb{R}})$ scales the (symmetric) particles farthest from the origin to unit distance. Let $C_{\bar{n}}\langle\mathbb{R}_\bullet\rangle$ and $C_{\bar{n}}\langle\mathbb{R}_o\rangle$ denote spaces where particles of $C_{\bar{n}}(\mathbb{R}_\bullet)/\text{Aff}(\bar{\mathbb{R}})$ and $C_{\bar{n}}(\mathbb{R}_o)/\text{Aff}(\bar{\mathbb{R}})$ have collided, respectively.

Proposition 3.5. $C_{\bar{n}}\langle\mathbb{R}_\bullet\rangle$ and $C_{\bar{n}}\langle\mathbb{R}_o\rangle$ have the same cellulation as \mathcal{CB}_n and \mathcal{CD}_n respectively.

Proof. From the above definition above, it is clear $C_{\bar{n}}(\mathbb{R}_\bullet)$ and $C_{\bar{n}}(\mathbb{R}_o)$ are complements of the hyperplanes given in Table 1. Thus any collision of particles in the configuration space maps to a point on the hyperplanes defined by the associated finite reflection group. Quotienting by $\text{Aff}(\bar{\mathbb{R}})$ allows choosing a particular representative for each fiber. Specifically, for the fiber containing (x_1, x_2, \dots, x_n) , choose

$$(x_1, x_2, \dots, x_n) / \sqrt{x_1^2 + x_2^2 + \dots + x_n^2},$$

giving a map onto the unit sphere in \mathbb{R}^n . The cellulation of the sphere by these hyperplanes yields the desired Coxeter complex. \square

¹The space $C_n\langle\mathbb{R}\rangle$ can also be thought of as the *closure* of $C_n(\mathbb{R})/\text{Aff}(\mathbb{R})$, though the space in which this closure is taken is non-trivial. An excellent treatment of these ideas in a general context is given by Sinha [30, Section 3].

3.2. We move from the spherical to the affine (toroidal) complexes. However, the interest now is on configurations of particles on the circle \mathbb{S} . The group of rotations acts freely on $C_n(\mathbb{S})$, and its quotient is denoted by $C_n(\mathbb{S}')$; Figure 3(a) shows a point in $C_9(\mathbb{S}')$ drawn without labels.

Proposition 3.6. $C_n(\mathbb{S}')$ has the same cellulation as $\mathrm{TC}\tilde{A}_{n-1}$.

A proof of this is given in [11, Section 3]. A similar construction is produced below for the other three toroidal Coxeter complexes. Our focus now is on the circle \mathbb{S} with the vertical line through its center as its axis of symmetry, where the two diametrically opposite points on the axis are labeled 0 and 1. The space of interest is the configuration space of pairs of *symmetric* labeled particles (again denoted \bar{n}) across this symmetric axis of the circle.

Definition 3.7. Let $C_{\bar{n}}(\mathbb{S}_\circ^\bullet) = \mathbb{T}^n - \{(x_1, x_2, \dots, x_n) \in \mathbb{T}^n \mid \exists i, j, x_i = \pm x_j \text{ or } x_i = 1\}$ be the space of n pairs of symmetric labeled particles on \mathbb{S} with a fixed particle at 1. Figure 3(b) shows a point in $C_{\bar{5}}(\mathbb{S}_\circ^\bullet)$.

Definition 3.8. Let $C_{\bar{n}}(\mathbb{S}_\bullet^\bullet) = \mathbb{T}^n - \{(x_1, x_2, \dots, x_n) \in \mathbb{T}^n \mid \exists i, j, x_i = \pm x_j \text{ or } x_i = 1 \text{ or } x_i = 0\}$ be the space of n pairs of symmetric labeled particles on \mathbb{S} with a fixed particle at 0 and 1. Figure 3(c) shows a point in $C_{\bar{5}}(\mathbb{S}_\bullet^\bullet)$.

Definition 3.9. Let $C_{\bar{n}}(\mathbb{S}_\circ^\circ) = \mathbb{T}^n - \{(x_1, x_2, \dots, x_n) \in \mathbb{T}^n \mid \exists i, j, x_i = \pm x_j\}$ be the space of n pairs of symmetric labeled particles on \mathbb{S} with no fixed particles. Figure 3(d) shows a point in $C_{\bar{5}}(\mathbb{S}_\circ^\circ)$.

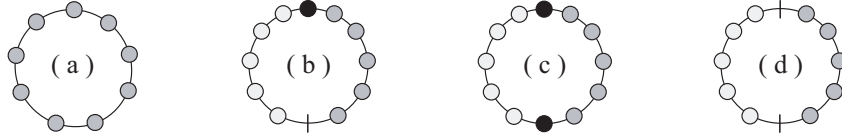


FIGURE 3. Configurations of particles (a) without and (b) - (d) with symmetry.

Proposition 3.10. $C_{\bar{n}}(\mathbb{S}_\circ^\bullet)$, $C_{\bar{n}}(\mathbb{S}_\bullet^\bullet)$ and $C_{\bar{n}}(\mathbb{S}_\circ^\circ)$ have the same cellulation as $\mathrm{TC}\tilde{B}_n$, $\mathrm{TC}\tilde{C}_n$ and $\mathrm{TC}\tilde{D}_n$ respectively.

Proof. This is a direct consequence of the definitions of the configuration spaces, of the toroidal complexes, and their corresponding hyperplane arrangements given in Table 2. \square

3.3. The group of reflections W across the respective hyperplanes acts on the configuration space by permuting particles. The Coxeter group A_n (the symmetric group) is generated by transpositions s_{ij} which interchange the i -th and j -th particle. The Coxeter group B_n of *signed permutations* is generated by s_{ij} along with reflections r_1, \dots, r_n , where r_i changes the sign of the i -th particle. Note that B_n is isomorphic to $\mathbb{Z}_2^n \rtimes \mathbb{S}_n$. The Coxeter group D_n is classically represented as the group of *even* signed permutations. Alternatively, D_n is isomorphic to the group $\mathbb{Z}_2^{n-1} \rtimes \mathbb{S}_n$, generated by transpositions s_{ij} along with reflections r_2, \dots, r_n . The element r_1 , which is present in B_n but not in D_n , corresponds to the reflection of the particle and its inverse that is closest to the origin.

Let $\sigma(W)$ denote the group acting *simply transitively* on the configuration spaces above. As mentioned above, for the spherical Coxeter groups, $\sigma(W)$ is isomorphic to W . However, the action of the affine groups is only transitive on the toroidal complexes. The simplest way to compute $\sigma(W)$ for the toroidal cases is from observing the diagrams given in Figure 3. Cutting the circle along a fixed point and “laying it flat” gives us the appropriate groups. Since a particle in $C_n(\mathbb{S}^1)$ is fixed by the group of rotations, then $\sigma(\tilde{A}_n)$ is isomorphic to A_{n-1} . Similarly, $\sigma(\tilde{B}_n)$ is isomorphic to D_n and $\sigma(\tilde{C}_n)$ is isomorphic to B_n . The group $\sigma(\tilde{D}_n)$ is isomorphic to $\mathbb{Z}_2^{n-2} \times \mathbb{S}_n$, generated by transpositions s_{ij} along with reflections r_2, \dots, r_{n-1} . The elements r_1 and r_n , which are not present in $\sigma(\tilde{D}_n)$, correspond to the reflections of the particles and their inverses that are closest to the centrally symmetric axis.

4. BRACKETINGS AND HYPERPLANES

4.1. We introduce the bracket notation in order to visualize collisions in the configuration spaces, leading to a transparent understanding of our results below. In particular, Proposition 4.4 produces a complete classification of the minimal building sets for the Coxeter complexes, along with their enumeration, as given in Tables 3 and 4.

A *bracket* is drawn around adjacent particles on a configuration space diagram representing the collision of the included particles. A *k-bracketing* of a diagram is a set of k brackets representing multiple independent particle collisions. For example, the configuration

$$(4.1) \quad -x_4 = -x_3 < -x_2 < -x_1 = 0 = x_1 < x_2 < x_3 = x_4$$

in $C_5(\mathbb{R}_\bullet)$ corresponds to the bracketing . Each bracket on a configuration space diagram with symmetric particles will actually consist of two symmetric brackets, one on each side of the origin, with this symmetric pair counting as only one bracket. If this set includes the origin, we draw one symmetric bracket around the origin, which again counts as one bracket. Thus Eq.(4.1) is a 2-bracketing of its diagram.

Let α be an intersection of hyperplanes. We say that hyperplanes h_i *cellulate* α to mean the intersections $h_i \cap \alpha$ decompose α into cells. Denote by $\mathcal{H}_s \alpha$ the set of all hyperplanes that contain α , called the stabilizing hyperplanes of α . If reflections in these hyperplanes generate a finite reflection group, it is called the *stabilizer* of α . Note that in a simplicial Coxeter complex, the stabilizer exists for all intersections of hyperplanes.²

We define the *support* of a bracketing to be the configuration space associated to the bracketing diagram. That is, it is the subspace (of the configuration space) in which particles that share a bracket have collided. However, a set of collisions in a configuration space defines an intersection of hyperplanes. So, alternatively, the support of a bracketing is the smallest intersection of hyperplanes associated to the bracketing. The following is immediate:

Lemma 4.1. *If α is the support of a bracketing G , then for every pair of particles x_i and x_j that share a bracket in G , the hyperplane defined by $x_i = x_j$ is in $\mathcal{H}_s \alpha$.*

²By abuse of terminology, we also refer to the set $\mathcal{H}_s \alpha$ as the stabilizer of α .

Example 4.2. Figure 4 shows part of the two-dimensional complexes \mathcal{CB}_3 and \mathcal{CD}_3 , one with and one without a fixed particle at the axis of symmetry. As we move through the chambers, going from (a) through (g), a representative of each configuration is shown. Notice that since there is no fixed particle at the axis of symmetry for type D , there is no meaningful bracketing of the symmetric particles closest to the axis; they may pass each other freely *without* collision.

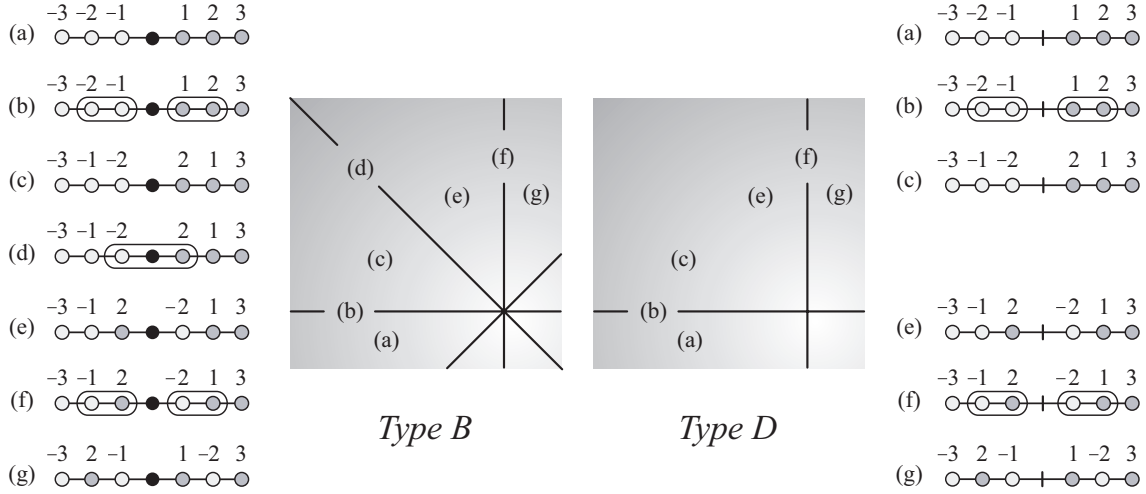


FIGURE 4. Local regions of \mathcal{CB}_3 and \mathcal{CD}_3 .

4.2. There are natural composition maps on bracketed diagrams. These form the basic operations of our operads defined in Section 5.

Definition 4.3. There are three types of compositions:

- (1) Let H be a diagram of m particles of $C_k(\mathbb{R})$ or $C_k(\mathbb{S}^1)$, with one particle labeled i . Let G be a diagram of $C_k(\mathbb{R})$. The *composition* $H \circ_i G$ is the diagram of $m + k - 1$ particles where the particle i is replaced by a bracket containing G .
- (2) Let H be a diagram of m paired particles of a configuration space, with one particle labeled i and its mirror image labeled $-i$. Let G be a diagram of $C_k(\mathbb{R})$. The *composition* $H \circ_i G$ is the diagram of $m + k - 1$ paired particles, where the particle i is replaced by a bracket containing G and its pair $-i$ is replaced by a bracket containing the mirror image of G (left side of Figure 5).

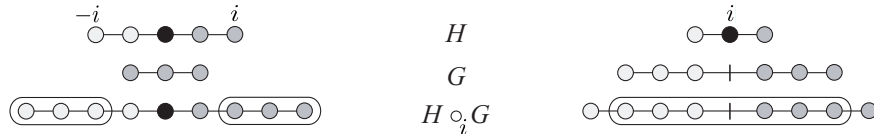


FIGURE 5. Composition operations on bracketings.

- (3) Let H be a diagram of m paired particles of $C_{\bar{m}}(\mathbb{R}_{\bullet})$, $C_{\bar{m}}(\mathbb{S}_{\circ}^{\bullet})$ or $C_{\bar{m}}(\mathbb{S}_{\circ}^{\bullet})$, with a fixed particle labeled i . Let G be a diagram of either $C_{\bar{k}}(\mathbb{R}_{\bullet})$ or $C_{\bar{k}}(\mathbb{R}_{\circ})$. The *composition* $H \circ_i G$ is the diagram of $m+k$ paired particles where the fixed particle i is replaced by a bracket containing G (right side of Figure 5).

Indeed any k -bracketing G can be represented as

$$(4.2) \quad G = H \circ_{i_1} G_1 \circ_{i_2} \cdots \circ_{i_k} G_k,$$

where the base H and the G_i 's are diagrams without brackets and each i_j is a particle in H .

Proposition 4.4. *Let G be a k -bracketing as defined in Eq.(4.2). Moreover, let α be the support of G and let α_i be the support of G_i . Then the stabilizer of α is the product of the stabilizers of α_i and the cellulation of α is determined by H .*

Proof. The product structure of the stabilizer of α is a consequence of Lemmas 4.1. The cellulation of α is determined by the hyperplanes of α , which are simply the intersections of hyperplanes of CW with α . If the particles x_i and x_j share a bracket in α , then x_k cannot collide with x_j in α without also colliding with x_i . Geometrically, this property implies that the two hyperplanes $x_i = x_k$ and $x_j = x_k$ have the same intersection with α . Similarly, since x_i and x_j collide in all of α , the hyperplane $x_i = x_j$ plays no role in the cellulation of α . These two facts allow us to treat x_i and x_j as a single particle in G without changing the hyperplane arrangement. Repeating this process for all particles that share a bracket gives the desired result. \square

4.3. It is easy to check that in most cases the cellulations of subspaces (intersections of hyperplanes) in Coxeter complexes are indeed other (smaller dimensional) Coxeter complexes. There are, however, three instances where this is not so, appearing as subspaces of the Coxeter complexes CD_n , $\mathbb{TC}\tilde{B}_n$ and $\mathbb{TC}\tilde{D}_n$. In particular, they have cellulations combinatorially equivalent to Coxeter complexes with *additional* hyperplanes. We define these three atypical complexes below:

Definition 4.5. The complexes of interest are:

1. Let $CD_{n,m}$ be CD_n with m additional hyperplanes $\{x_i = 0 \mid 1 \leq i \leq m\}$.
2. Let $\mathbb{TC}\tilde{B}_{n,m}$ be $\mathbb{TC}\tilde{B}_n$ with m additional hyperplanes $\{x_i = 0 \mid 1 \leq i \leq m\}$.
3. Let $\mathbb{TC}\tilde{D}_{n,m}$ be $\mathbb{TC}\tilde{D}_n$ with $2m$ additional hyperplanes $\{x_i = 0, 1 \mid 1 \leq i \leq m\}$.

The configuration space model provides intuition into how these cases arise naturally. Note how these are all complexes with associated configuration spaces on \mathbb{R}_{\circ} , $\mathbb{S}_{\circ}^{\bullet}$ and $\mathbb{S}_{\circ}^{\circ}$, where not all points along the axis of symmetry have fixed particles. The subspaces of these configuration spaces are those where some particles have collided. In these subspaces, sets of collided particles may be considered in aggregate as a new type of particle, called a *thick* particle. Figure 6(a) shows a bracketing and (b) its representation with thick particles. In general, thick particles allow us to represent any number of coincident particles by a single particle.

Recall that particles were defined such that they could occupy the same point as their inverse; that is, they do not form a collision with their inverse. Unlike (standard) particles, a thick particle and its inverse may not occupy the same point without collision. The reason comes from the

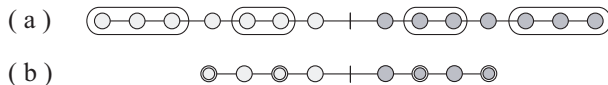


FIGURE 6. Bracketing and thick particles.

hyperplane equations: In the subspace where x_i and x_j have collided, the hyperplane $x_i = -x_j$ represents the same configurations as $x_i = -x_i (= 0)$. Thus, the m additional hyperplanes added to the complex correspond to the m thick particles in their configuration spaces. Then the diagram of Figure 6(b) is an element of $\mathcal{CD}_{4,2}$, sitting as a subspace of \mathcal{CD}_7 in Figure 6(a).

Remark. In the case of non-paired particles, the distinction between standard and thick particles is irrelevant, since no particle has an inverse to collide with. They are also inconsequential in configuration spaces that include a fixed particle wherever particles may meet their inverses.

5. COMPACTIFICATIONS AND OPERADS

5.1. Compactifying a configuration space $C_n(V)$ enables the points on V to collide and a *system* is introduced to record the *directions* points arrive at the collision. In the work of Fulton and MacPherson [16], this method is brought to rigor in the algebro-geometric context.³ In [9, Section 4], De Concini and Procesi show that the *minimal blow-ups* of the Coxeter complexes CW are equivalent to the Fulton-MacPherson compactifications of their corresponding configuration spaces.

In order to describe these compactified Coxeter moduli spaces, we begin with definitions. The collection of hyperplanes $\{x_i = 0 \mid i = 1, \dots, n\}$ of \mathbb{R}^n generates the *coordinate* arrangement. A crossing of hyperplanes is *normal* if it is locally isomorphic to a coordinate arrangement. A construction which transforms any crossing into a normal crossing involves the algebro-geometric concept of a blow-up; a standard reference is [18].

Definition 5.1. The *blow-up* of a space V along a codimension k intersection α of hyperplanes is the closure of $\{(x, f(x)) \mid x \in V\}$ in $V \times \mathbb{P}^{k-1}$. That is, we replace α with the projective sphere bundle associated to the normal bundle of α .

A general collection of blow-ups is usually noncommutative in nature; in other words, the order in which spaces are blown up is important. For a given arrangement, De Concini and Procesi [9, Section 3] establish the existence and uniqueness of a *minimal building set*, a collection of subspaces for which blow-ups commute for a given dimension, and for which every crossing in the resulting space is normal. For a Coxeter complex CW , we denote the minimal building set by $\text{Min}(CW)$.

Definition 5.2. The *Coxeter moduli space* $\mathcal{C}(W)_\#$ is the minimal blow-up of CW , obtained by blowing up along elements of $\text{Min}(CW)$ in *increasing* order of dimension.

Remark. Kapranov showed the minimal blow-ups of \mathcal{CA}_n yield a space homeomorphic to a double cover of the moduli space $\overline{\mathcal{M}}_{0,n+2}(\mathbb{R})$ [19, Proposition 4.8]. Thus, the Fulton-MacPherson compactifications of our configuration spaces yield generalizations of this moduli space.

³Axelrod and Singer [1] look at this compactification from a perspective of spherical blow-ups on real manifolds.

Example 5.3. Figure 7(a) shows the blow-ups of the sphere \mathcal{CA}_3 of Figure 2(a) at nonnormal crossings. Each blown up point has become a hexagon with antipodal identification and the resulting manifold is the Coxeter moduli space $\mathcal{C}(A_3)_\#$, homeomorphic to the eight-fold connected sum of \mathbb{RP}^2 with itself.⁴ Part (b) shows $\overline{\mathcal{M}}_{0,6}(\mathbb{R})$ coming from the iterated blow-ups of \mathcal{CA}_4 . Figure 7(c) shows the minimal blow-up of $\mathcal{C}\tilde{A}_2$ of Figure 2(e). Finally, part (d) is the cube with opposite facial identifications yielding the three-torus of $\mathcal{C}(\tilde{A}_3)_\#$.

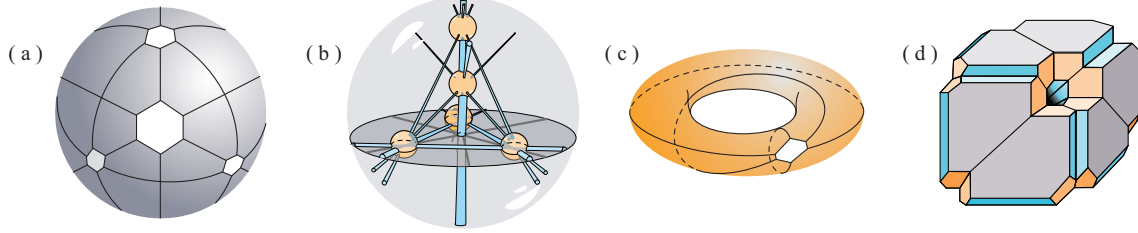


FIGURE 7. Coxeter moduli spaces (a) $\mathcal{C}(A_3)_\#$, (b) $\mathcal{C}(A_4)_\#$, (c) $\mathcal{C}(\tilde{A}_2)_\#$ and (d) $\mathcal{C}(\tilde{A}_3)_\#$.

The relationship between the set $\text{Min}(CW)$ and the group W is given by the concept of reducibility. For intersections of hyperplanes α, β , and γ , the collection of hyperplanes $\mathcal{H}_s\alpha$ is *reducible* if $\mathcal{H}_s\alpha$ is a disjoint union $\mathcal{H}_s\beta \sqcup \mathcal{H}_s\gamma$, where $\alpha = \beta \cap \gamma$.

Lemma 5.4. [8, Section 3] *Let α be an intersection of hyperplanes of CW . Then $\mathcal{H}_s\alpha$ is irreducible if and only if α is in $\text{Min}(CW)$.*

This lemma can be rewritten in the language of bracketings:

Lemma 5.5. *Let α be an intersection of hyperplanes of CW . Then α is in $\text{Min}(CW)$ if and only if α is the support of a 1-bracketing.*

Proof. If α is the support of a 1-bracketing G , then $\mathcal{H}_s\alpha$ is determined by Lemma 4.1. Thus:

- (1) If G contains a fixed particle, then $\mathcal{H}_s\alpha \cong \mathcal{HB}_k$.
- (2) If G contains a particle and its inverse but no fixed particle, then $\mathcal{H}_s\alpha \cong \mathcal{HD}_k$.
- (3) If G does not contain a particle and its inverse, then $\mathcal{H}_s\alpha \cong \mathcal{HA}_k$.

All three of these hyperplane arrangements are irreducible, so α is in $\text{Min}(CW)$.

Conversely, let α be the support of a k -bracketing $G = H \circ_{i_1} G_1 \circ_{i_2} \cdots \circ_{i_k} G_k$. Let β be the support of G_1 and γ be the product of the configuration spaces diagramed by G_2, \dots, G_k . By the definition of reducibility, $\mathcal{H}_s\alpha = \mathcal{H}_s\beta \sqcup \mathcal{H}_s\gamma$, and thus α is not in $\text{Min}(CW)$ by Lemma 5.4. \square

Remark. Table 3 itemizes the collection of elements in $\text{Min}(CW)$ for the spherical cases and Table 4 for the Euclidean ones. In the tables, m represents the total number of thick particles and r the number of thick particles in the bracket (stabilizer) of the atypical complexes.

⁴A projective version of this diagram is first found in a different context by Brahana and Coble in 1926 [5, Section 1] relating to possibilities of maps with twelve five-sided countries.

5.2. As bracketings encoded collisions of particles in configuration spaces, it is *nested* bracketings which encode the Fulton-MacPherson compactification of the configuration spaces [9, Section 2]. The FM compactification allows collisions of particles whose description comes from the repulsive potential observed by quantum physics: Pushing particles together creates a spherical bubble onto which the particles escape [25]. In other words, as particles try to collide, the result is a new bubble fused to the old at the point of collision, where the collided particles are now on the new bubble. The phenomena is dubbed as *bubbling*, with the resulting structure as a bubble-tree. Indeed, the nested bracketings are exactly the one-dimensional analogues of bubble-trees [10, Section 1].

Moreover, the codimension k faces of a chamber of a compactified configuration space are the nested k -bracketings on the configuration space diagrams. A diagram G denoted

$$(5.1) \quad G = H \circ_{i_1} G_1 \circ_{i_2} \cdots \circ_{i_k} G_k,$$

is a nested $(k + m_0 + m_1 + \cdots + m_k)$ -bracketing, with each i_j a particle of H , where H is an m_0 -bracketing and where G_i is a nested m_i -bracketing; see Figure 8. The composition maps are those in Definition 4.3.

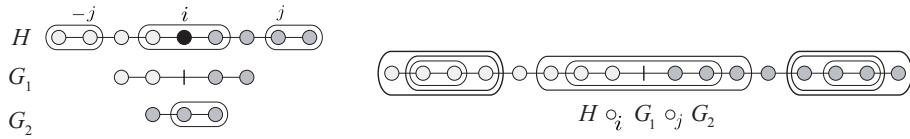


FIGURE 8. Composition operations on nested bracketings.

After compactification, different orderings of particles in a bracket do not necessarily represent the same cell. A different action is necessary to describe the identification of diagrams.

Definition 5.6. The *flip* $\hat{\sigma}(G)$ action on an unbracketed diagram G consists of the identity and the reflection (that reverses the order of the particles of G). On a nested bracketing diagram, the action of $\hat{\sigma}(G)$ acts independently on each bracketed component.

Theorem 5.7. *Let G be a nested bracketing where $G = H \circ_{i_1} G_1 \circ_{i_2} \cdots \circ_{i_k} G_k$. All bracketings in the image of G under $\hat{\sigma}(G_1) \times \cdots \times \hat{\sigma}(G_k)$ represent the same cell.*

Proof. By definition, blow-ups introduce a *projective* bundle around each subspace in the minimal building set. The analog in configuration spaces is an identification across each bracket: Flipping the positions of the particles in the bracket is defined to represent the same configuration. Thus the permutations that represent the same set of configurations as G are exactly the images of G under $\hat{\sigma}(G_1) \times \cdots \times \hat{\sigma}(G_k)$. \square

Remark. This theorem gives us a gluing rule between the faces of two chambers. In other words, two nested k -bracketings G_1 and G_2 of a diagram (representing codimension k -faces) are identified if G_2 can be obtained from G_1 by flipping some of the brackets of G_2 .

Figure 9 shows the permutations that preserve the cell represented by a particular configuration space diagram. Note that reflections commute with each other, and thus they generate a group which is isomorphic to $(\mathbb{Z}/2\mathbb{Z})^3$.

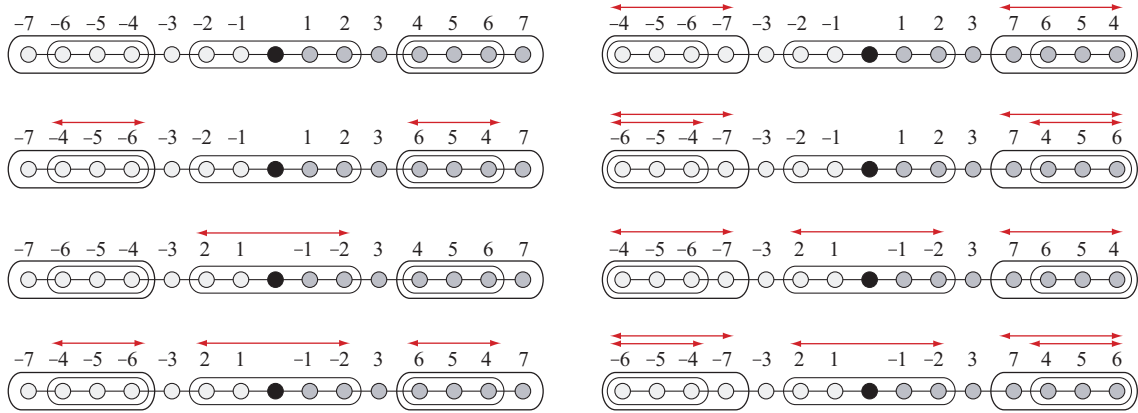


FIGURE 9. Flips on nested bracketings.

5.3. Classically, the notion of an operad was created for the study of iterated loop spaces [32]. Since then, operads have been used as universal objects representing a wide range of algebraic concepts. An *operad* \mathcal{O} consists of a collection of objects $\{\mathcal{O}(n) \mid n \in \mathbb{N}\}$ in a monoidal category endowed with certain extra structures. Notably, $\mathcal{O}(n)$ carries an action by the symmetric group of n letters, and there are composition maps

$$\mathcal{O}(n) \otimes \mathcal{O}(k_1) \otimes \cdots \otimes \mathcal{O}(k_n) \rightarrow \mathcal{O}(k_1 + \cdots + k_n)$$

which must be associative, unital, and equivariant; see [22, Chapter 1] for details.

One can view $\mathcal{O}(n)$ as objects consisting of n -ary operations, which yield an output given n inputs. We will be concerned mostly with operads in the context of topological spaces, where the objects $\mathcal{O}(n)$ will be equivalence classes of geometric objects. Classically, these objects can be pictured as in Figure 10. The composition $\mathcal{O}(i) \circ_k \mathcal{O}(j)$ is obtained by grafting the output of $\mathcal{O}(j)$ to the k -th input of $\mathcal{O}(i)$. The symmetric group acts by permuting the labeling of the inputs.

There are several variants and extensions of the operad definition above. A classic example is the *non-symmetric* version, which removes all references to the symmetric group in the definition above. A *right module* \mathcal{O}_R over an operad \mathcal{O} is a collection of objects $\{\mathcal{O}_R(n) \mid n \in \mathbb{N}\}$ with a set of composition maps

$$\mathcal{O}_R(n) \otimes \mathcal{O}(k_1) \otimes \cdots \otimes \mathcal{O}(k_n) \rightarrow \mathcal{O}_R(k_1 + \cdots + k_n).$$

A *bi-colored* operad is a multicategory with two objects [23, Section 2]: Intuitively, each of the inputs and output is given one of two colors. An element $\mathcal{O}(j)$ can be grafted into an input of $\mathcal{O}(i)$ if and only if the colors of the corresponding input and output match. Our version (the naming of which is credited to J. Stasheff) replaces the symmetric group in the classical definition with appropriate Coxeter groups instead. Let Ω be the collection $\{A, B, D, \tilde{A}, \tilde{B}, \tilde{C}, \tilde{D}\}$ of Coxeter groups from Figure 1.

Definition 5.8. For $W \in \Omega$, let $\mathcal{O}_W(n, k)$ be the collection of configuration spaces of nested k -bracketings with n particles associated to $\mathcal{C}(W)_\#$. If \mathcal{U} is a subset of Ω , then let $\mathcal{O}_\mathcal{U} = \bigcup_{W \in \mathcal{U}} \mathcal{O}_W$. Then, the *Coxeter operad* is defined for each pair \mathcal{U}, \mathcal{V} of (possibly empty) subsets of Ω for which

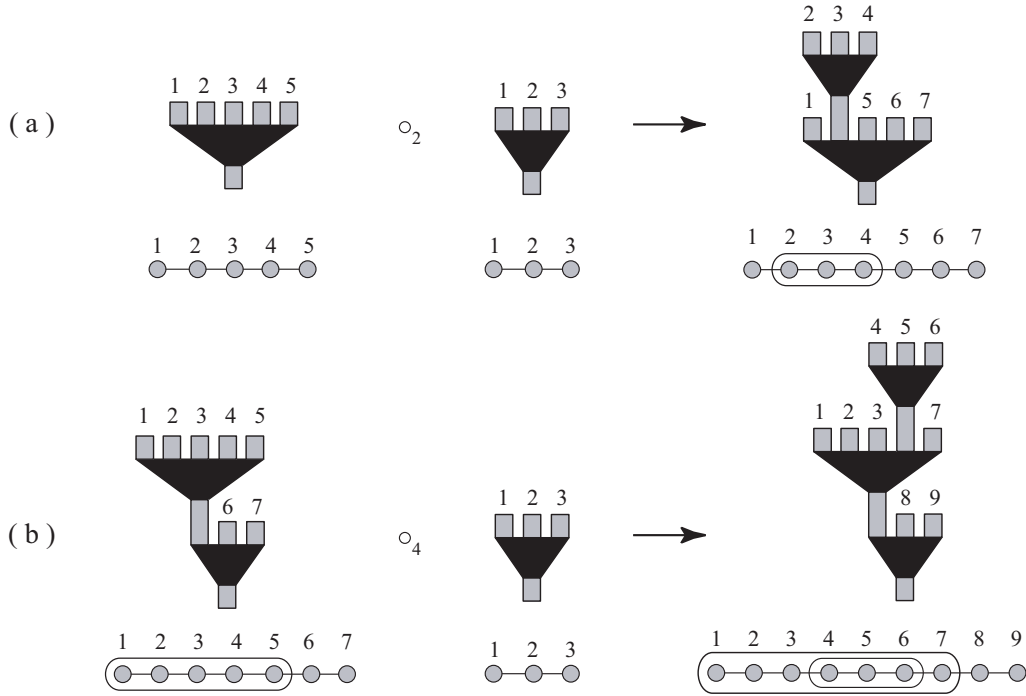


FIGURE 10. Examples of composition maps of an operad, along with dual figures related to (a) bracketing and (b) nested bracketing.

the collection

$$\mathcal{O}_U(n_H, k_H) \otimes \mathcal{O}_V(n_1, k_1) \otimes \cdots \otimes \mathcal{O}_V(n_m, k_m) \rightarrow \mathcal{O}_U(n_*, k_*)$$

of composition maps exist, where $n_* = n_H - m + \sum n_i$ and $k_* = k_H + m + \sum k_i$.

We note several structures that appear based on this definition, giving a partial list:

Classic Operads: When $\mathcal{U} = \mathcal{V} = \{A\}$, the Coxeter operad becomes the A_∞ operad structure [32] of the associahedron. The classic symmetric group acting on \mathcal{O}_A is exactly the A_n Coxeter group. Examples of this are seen in Figure 10.

Right Modules: When $\mathcal{V} = \{A\}$ and $\mathcal{U} = \{W\}$, for any $W \in \Omega \setminus A$, we have a right module \mathcal{O}_W over the operad \mathcal{O}_A . The composition map (based on non-nested bracketings) is described in Definition 4.3 (2) for centrally symmetric spaces. Moreover, Definition 4.3 (1) provides the composition for $W = \tilde{A}$, resulting in the cyclohedron structure given in [22, Section 4.4].

Bi-Colored Operads: When $\mathcal{U} = \{B\}$ and $\mathcal{V} = \{A, B, D\}$, we obtain a bi-colored operad. The two colors come from the centrally symmetric black particle and the ordinary free particles. The map for $D \in \mathcal{V}$ is diagrammed in the top part of Figure 11, whereas the map for $A \in \mathcal{V}$ is given in the bottom of the figure. This composition map is described in Definition 4.3 (3).

Bi-Colored Right Modules: The examples where $\mathcal{U} = \{\tilde{B}, \tilde{C}, \tilde{D}\}$ and $\mathcal{V} = \{A, B, D\}$ result in the composition of bracketings on line being glued onto bracketings on circles. This results in a bi-colored right module over a bi-colored operad. There are several options here which work for the different subsets of \mathcal{U} and \mathcal{V} given. For example, $\mathcal{O}_{\tilde{D}}$ admits an action of \mathcal{O}_A and $\mathcal{O}_{\{\tilde{B}, \tilde{C}\}}$ admits an action of $\mathcal{O}_{\{B, D\}}$. From an operadic viewpoint, the affine Coxeter groups are analogous to the spherical ones shown, but an *unrooted tree*, rather than a rooted one, is used.

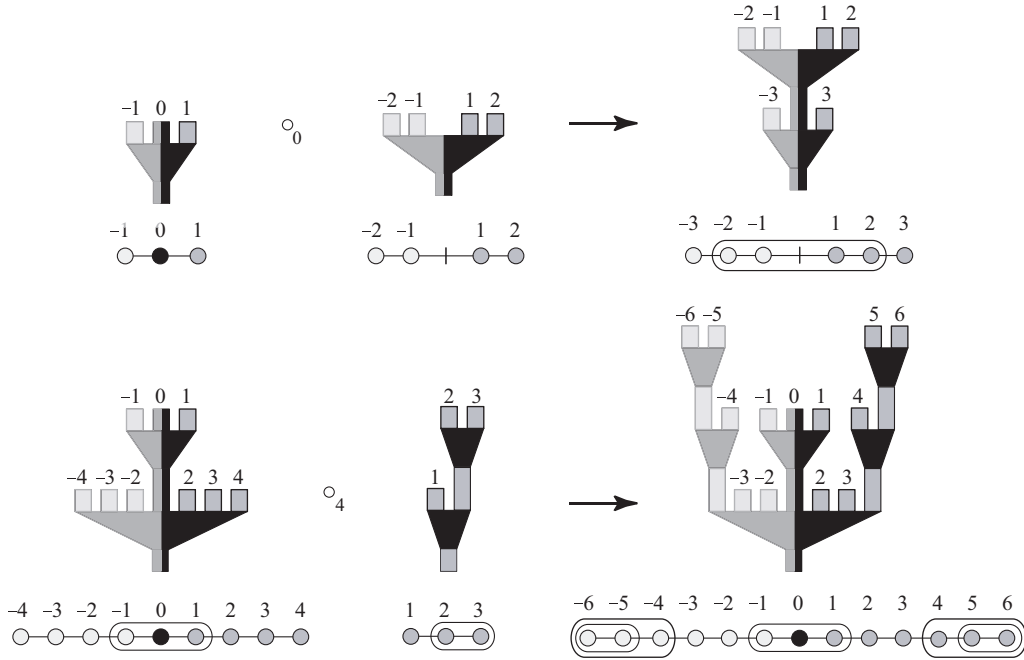


FIGURE 11. Examples of composition maps of the Coxeter operad, along with dual *tree* figures.

Remark. There exists a generalization of the classical operad to the *braid* operad, defined by Fiedorowicz, with the braid group playing the role of the symmetric group [14, Section 3]. Since the braid group is the Artin group of type A , it seems plausible that the Coxeter operads above can be extended to their corresponding Artin groups, yielding analogs to the braid operads.

6. TILING BY GRAPH-ASSOCIAHEDRA

6.1. This section uses the theory of graph-associahedra developed in [6]. As associahedra are related to the A_∞ operad, we show that graph-associahedra capture the structure of the Coxeter operad. Moreover, we provide combinatorial and enumerative results about the Coxeter moduli spaces. Notably, the Euler characteristics of these spaces are given.

Definition 6.1. Let Γ be a graph. A *tube* is a proper nonempty set of nodes of Γ whose induced graph is a proper, connected subgraph of Γ . There are three ways that two tubes t_1 and t_2 may interact on the graph.

- (1) Tubes are *nested* if $t_1 \subset t_2$.
- (2) Tubes *intersect* if $t_1 \cap t_2 \neq \emptyset$ and $t_1 \not\subset t_2$ and $t_2 \not\subset t_1$.
- (3) Tubes are *adjacent* if $t_1 \cap t_2 = \emptyset$ and $t_1 \cup t_2$ is a tube in Γ .

Tubes are *compatible* if they do not intersect and they are not adjacent. A *tubing* T of Γ is a set of tubes of Γ such that every pair of tubes in T is compatible. A k -*tubing* is a tubing with k tubes.

Theorem 6.2. [6, Section 3] *For a graph Γ with n nodes, the graph-associahedron $\mathcal{P}\Gamma$ is the convex polytope of dimension $n - 1$ whose face poset is isomorphic to set of valid tubings of Γ , ordered such that $T \prec T'$ if T is obtained from T' by adding tubes.*

Figure 12 shows two examples of graph-associahedra, having underlying graphs as paths and cycles, respectively, with three nodes. These turn out to be the two-dimensional associahedron [32] and cyclohedron [3] polytopes.

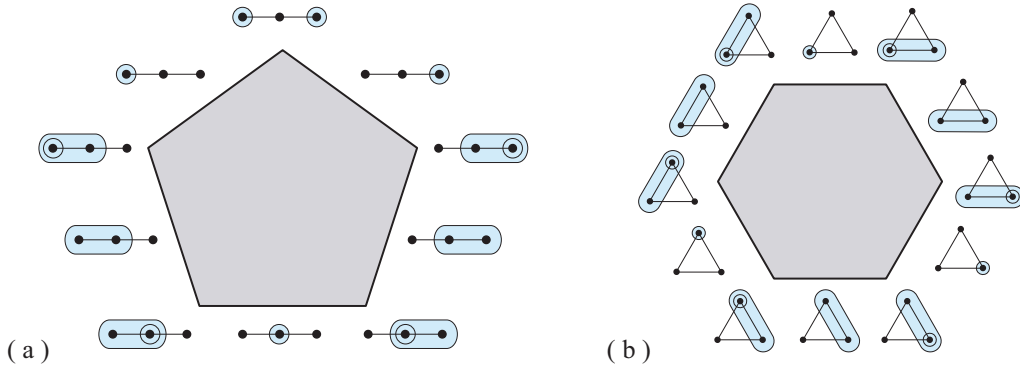


FIGURE 12. Graph-associahedra with a (a) path and (b) cycle as underlying graphs.

Theorem 6.3. [6, Section 4] *Let W be a simplicial Coxeter group and Γ_W be its associated Coxeter graph. Then the W -action on $CW_\#$ has a fundamental domain combinatorially isomorphic to $\mathcal{P}\Gamma_W$.*

Notation. We write $\mathcal{P}W$ instead of $\mathcal{P}\Gamma_W$ when context makes it clear.

Theorem 6.4. *The tiling of the Coxeter moduli spaces are given as follows:*

- (1) $\mathcal{P}A_n$ (the associahedron) tiles $\mathcal{C}(A_n)_\#$, $\mathcal{C}(B_n)_\#$ and $\mathbb{TC}(\tilde{C}_{n-1})_\#$.
- (2) $\mathcal{P}\tilde{A}_n$ (the cyclohedron) tiles $\mathbb{TC}(\tilde{A}_n)_\#$.
- (3) $\mathcal{P}D_n$ tiles $\mathcal{C}(D_n)_\#$ and $\mathbb{TC}(\tilde{B}_{n-1})_\#$.
- (4) $\mathcal{P}\tilde{D}_n$ tiles $\mathbb{TC}(\tilde{D}_n)_\#$.

Proof. For a given graph Γ , the polytope $\mathcal{P}\Gamma_n$ depends only on the adjacency of nodes, not the label on the edges. \square

Remark. There is a natural bijection from the set of all bracketings of a configuration space diagram to the set of all tubings of the associated Coxeter diagram. The bijection is such that two brackets intersect if and only if their images intersect or are adjacent as tubes. Thus the face poset of tubings

is isomorphic to the face poset of bracketings, where k brackets correspond to a codimension k face. Figure 13 shows some examples of this bijection.

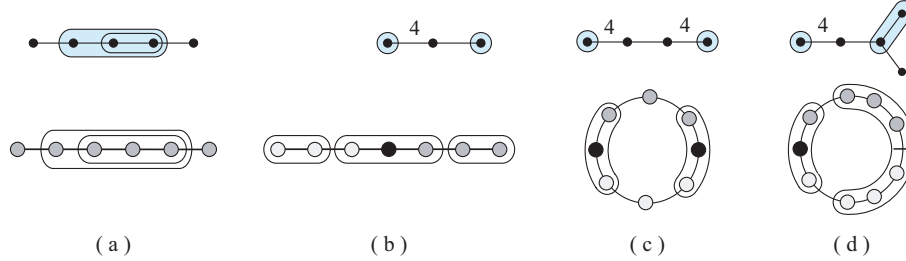


FIGURE 13. Examples of the bijection between tubings and nested bracketings.

6.2. We analyze the structure of these tiling polyhedra \mathcal{PW} . For a given tube t and a graph Γ , let Γ_t denote the induced subgraph on the graph Γ . By abuse of notation, we sometimes refer to Γ_t as a tube.

Definition 6.5. Given a graph Γ and a tube t , construct a new graph Γ_t^* called the *reconnected complement*: If V is the set of nodes of Γ , then $V - t$ is the set of nodes of Γ_t^* . There is an edge between nodes a and b in Γ_t^* if either $\{a, b\}$ or $\{a, b\} \cup t$ is connected in Γ .

Theorem 6.6. [6, Section 3] *The facets of $\mathcal{P}\Gamma$ correspond to the set of 1-tubings on Γ . In particular, the facet associated to a 1-tubing $\{t\}$ is equivalent to $\mathcal{P}\Gamma_t \times \mathcal{P}\Gamma_t^*$.*

The facets of \mathcal{PW} are of the form $\mathcal{P}\Gamma \times \mathcal{P}\Gamma^*$, which can be found by simple inspection. Using induction on each term of the product produces the following results:

Corollary 6.7. [32] *The faces of \mathcal{PA} are of the form $\mathcal{PA} \times \cdots \times \mathcal{PA}$.*

Corollary 6.8. [33] *The faces of $\mathcal{P}\tilde{A}$ are of the form $\mathcal{P}\tilde{A} \times \mathcal{PA} \times \cdots \times \mathcal{PA}$.*

Before moving on to the other tiling polytopes, we need to look at some special graphs which appear as reconnected complements. They are displayed in the Figure 14 below, the subscript n denoting the number of vertices. Note that the polytope $\mathcal{P}X_4$ is the 3-dimensional *permutohedron*.

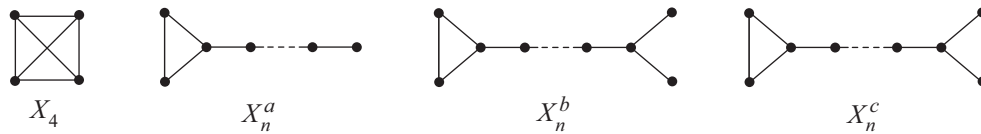


FIGURE 14. Special graphs appearing as reconnected complements.

Corollary 6.9. *The faces of \mathcal{PD} are of the form*

- (1) $\mathcal{PA} \times \cdots \times \mathcal{PA}$
- (2) $\mathcal{PD} \times \mathcal{PA} \times \cdots \times \mathcal{PA}$

$$(3) \mathcal{P}X^a \times \mathcal{P}A \times \cdots \times \mathcal{P}A.$$

Example 6.10. Figure 15 illustrates four different polyhedra. The first three are well-known objects: (a) the associahedron $\mathcal{P}A_4$, (b) cyclohedron $\mathcal{P}\tilde{A}_4$ and (c) permutohedron $\mathcal{P}X_4$. The last one (d) is $\mathcal{P}D_4$ with six pentagons $\mathcal{P}A_3$, three squares $\mathcal{P}D_2 \times \mathcal{P}A_2$ and one hexagon $\mathcal{P}X_3^g$ for facets.

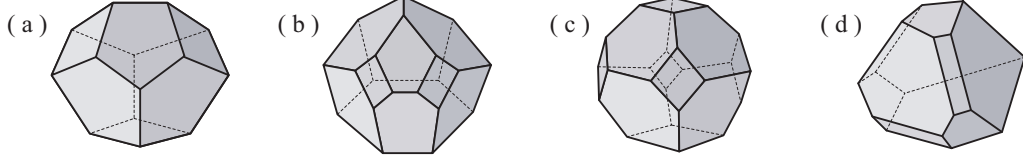


FIGURE 15. The 3-dimensional (a) associahedron $\mathcal{P}A_4$, (b) cyclohedron $\mathcal{P}\tilde{A}_3$, (c) permutohedron $\mathcal{P}X_4$ and (d) $\mathcal{P}D_4$.

Corollary 6.11. *The faces of $\mathcal{P}\tilde{D}$ are of the form*

- | | |
|--|--|
| (1) $\mathcal{P}A \times \cdots \times \mathcal{P}A$ | (6) $\mathcal{P}D \times \mathcal{P}D \times \mathcal{P}A \times \cdots \times \mathcal{P}A$ |
| (2) $\mathcal{P}D \times \mathcal{P}A \times \cdots \times \mathcal{P}A$ | (7) $\mathcal{P}X^b \times \mathcal{P}A \times \cdots \times \mathcal{P}A$ |
| (3) $\mathcal{P}X^a \times \mathcal{P}A \times \cdots \times \mathcal{P}A$ | (8) $\mathcal{P}X^c \times \mathcal{P}A \times \cdots \times \mathcal{P}A$ |
| (4) $\mathcal{P}X^a \times \mathcal{P}X^a \times \mathcal{P}A \times \cdots \times \mathcal{P}A$ | (9) $\mathcal{P}\tilde{D} \times \mathcal{P}A \times \cdots \times \mathcal{P}A$ |
| (5) $\mathcal{P}D \times \mathcal{P}X^a \times \mathcal{P}A \times \cdots \times \mathcal{P}A$ | (10) $\mathcal{P}X_4 \times \mathcal{P}A \times \cdots \times \mathcal{P}A$. |

6.3. We compute the Euler characteristics of the Coxeter moduli spaces. From Theorem 6.6, we see that the number of codimension k faces of the polytope $\mathcal{P}W$ cellulating $\mathcal{C}W_\#$ is precisely the number of k -tubings of the associated Coxeter diagram Γ_W .

Theorem 6.12. *Let $f_k(\mathcal{P}W)$ be the number of k -dimensional faces of $\mathcal{P}W$, and let g be the number of chambers in the spherical or toroidal Coxeter complex $\mathcal{C}W$. If $\dim(\mathcal{P}W) = n$, then*

$$\chi(\mathcal{C}(W)_\#) = \sum_{k=0}^n (-1)^k \frac{g \cdot f_k}{2^{n-k}}.$$

Proof. In order to count the number of k -dimensional faces in the space $\mathcal{C}(W)_\#$, take the number of total chambers g and multiply it by the number of k -dimensional faces $f_k(\mathcal{P}W)$ for each tile $\mathcal{P}W$. The amount of overcounting is simply how different chambers of the complex meet at each k -dimensional face of a tile. Since all the crossings in $\mathcal{C}(W)_\#$ are normal, each k -dimensional face is identified with 2^{n-k} copies. \square

Remark. The number of vertices in $\mathcal{P}A$ is the well-known Catalan number [31, Section 6.5]. The faces $f_k(W)$ of $\mathcal{P}W$ provide natural generalizations; see [26] for further exposition.

Theorem 6.4 shows only four types of graph-associahedra tiling the Coxeter moduli spaces: $\mathcal{P}A_n$ (the associahedron), $\mathcal{P}\tilde{A}_n$ (the cyclohedron), $\mathcal{P}D_n$ and $\mathcal{P}\tilde{D}_n$. The enumeration of the faces of the

associahedra $\mathcal{P}A_n$ is a classic result of A. Cayley [7], obtained by just counting the number of n -gons with k non-intersecting diagonals:

$$f_k(\mathcal{P}A_n) = \frac{1}{n+1} \binom{n-1}{k} \binom{2n-k}{n}.$$

The enumeration of the face poset of the cylohedron $\mathcal{P}\tilde{A}_n$ comes from Simion [29, Section 3]:

$$f_k(\mathcal{P}\tilde{A}_n) = \binom{n}{k} \binom{2n-k}{n}.$$

In a recent paper, Postnikov provides a recursive formula for the generating function of the numbers f_k [26, Theorem 7.11]. Using this, a closed formulas for the graph-associahedra of types D_n and \tilde{D}_n can be found; see [27, Section 12]. We thank A. Postnikov for sharing the following result:

Proposition 6.13. *The face poset enumerations of types D_n and \tilde{D}_n are*

$$(6.1) \quad f_k(\mathcal{P}D_n) = 2f_k(\mathcal{P}A_n) - 2f_k(\mathcal{P}A_{n-1}) - f_k(\mathcal{P}A_{n-2}) - f_{k-1}(\mathcal{P}A_{n-1}) - f_{k-1}(\mathcal{P}A_{n-2})$$

$$(6.2) \quad \begin{aligned} f_k(\mathcal{P}\tilde{D}_n) &= 4f_k(\mathcal{P}A_{n+1}) - 8f_k(\mathcal{P}A_n) - 4f_{k-1}(\mathcal{P}A_n) + f_{k-2}(\mathcal{P}A_{n-1}) \\ &+ 4f_k(\mathcal{P}A_{n-2}) + 6f_{k-1}(\mathcal{P}A_{n-2}) + 2f_{k-2}(\mathcal{P}A_{n-2}) \\ &+ f_k(\mathcal{P}A_{n-3}) + 2f_{k-1}(\mathcal{P}A_{n-3}) + f_{k-2}(\mathcal{P}A_{n-3}). \end{aligned}$$

Theorem 6.14. *The Euler characteristics of the spherical blown-up Coxeter complexes are as follows: When n is even, the values are zero; when $n = 2m + 1$ is odd,*

$$(6.3) \quad \chi(\mathcal{C}(A_n)_\#) = (-1)^m 2n ((n-2)!!)^2$$

$$(6.4) \quad \chi(\mathcal{C}(B_n)_\#) = 2^n \frac{1}{(n+1)} \chi(\mathcal{C}(A_n)_\#)$$

$$(6.5) \quad \chi(\mathcal{C}(D_n)_\#) = 2^{n-3} \left[\frac{8}{n+1} - \frac{1}{n-2} \right] \chi(\mathcal{C}(A_n)_\#).$$

The Euler characteristics of the toroidal blown-up Coxeter complexes are as follows: When n is odd, the values are zero; when $n = 2m$ is even,

$$(6.6) \quad \chi(\mathbb{T}\mathcal{C}(\tilde{A}_n)_\#) = (-1)^m ((n-1)!!)^2$$

$$(6.7) \quad \chi(\mathbb{T}\mathcal{C}(\tilde{B}_n)_\#) = \frac{1}{2(n+1)} \chi(\mathcal{C}(D_{n+1})_\#)$$

$$(6.8) \quad \chi(\mathbb{T}\mathcal{C}(\tilde{C}_n)_\#) = 2^n \frac{1}{(n+2)(n+1)} \chi(\mathcal{C}(A_{n+1})_\#)$$

$$(6.9) \quad \chi(\mathbb{T}\mathcal{C}(\tilde{D}_n)_\#) = 2^{n-6} \frac{1}{(n+1)} \left[\frac{64}{n+2} - \frac{15}{n-1} \right] \chi(\mathcal{C}(A_{n+1})_\#).$$

Proof. We use Theorem 6.12 to obtain a summation, using the values f_k given above along with the number of chambers provided by Tables 1 and 2. The values for Eqs.(6.3) and (6.6) have been previously calculated in [10, Section 3.2] and [29, Section 4.3] respectively. Equations (6.4), (6.7) and (6.8) are consequences of Theorem 6.4, where these spaces share the same tiling polytopes as

previous calculations. From Eq. (6.1) and Theorem 6.12, we obtain a linear combination

$$\begin{aligned} \chi(\mathcal{C}(D_n)_\#) &= \frac{2^n}{(n+1)!} \chi(\mathcal{C}(A_n)_\#) - \frac{2^{n-1}}{n!} \chi(\mathcal{C}(A_{n-1})_\#) - \frac{2^{n-3}}{(n-1)!} \chi(\mathcal{C}(A_{n-2})_\#) \\ &\quad + \frac{2^{n-1}}{n!} \chi(\mathcal{C}(A_{n-1})_\#) + \frac{2^{n-2}}{(n-1)!} \chi(\mathcal{C}(A_{n-2})_\#). \end{aligned}$$

Algebraic manipulations result in Eq.(6.5). Similar calculations using Eq. (6.2) yield Eq. (6.9) after simplification. \square

Remark. The reason there is a dimension shift between the spherical and toroidal cases is due to the convention of the affine case having $n+1$ nodes in its Coxeter graph, compared to n nodes for the spherical.

6.4. The polytopes tiling the Coxeter moduli spaces are given by Theorem 6.4. We now discuss the tiling of the atypical complexes, given in Definition 4.5, after minimal blow-ups. As in other (compactified) configuration spaces, the chambers of these complexes correspond to orderings of the particles. However, different orderings of particles may give different face posets to the chamber, since switching a standard and thick particle may change the valid bracketings of the diagram. Specifically, near an axis of symmetry with no fixed particles, having thick particles allows more collisions and hence more brackets, than having standard particles. It is here where the polytopes $\mathcal{P}X^a$, $\mathcal{P}X^b$, and $\mathcal{P}X^c$ based on Figure 14 appear.

Recall that the chambers of these complexes arise as subspaces of $\mathcal{C}(D_n)_\#$, $\mathcal{TC}(\tilde{B}_n)_\#$ or $\mathcal{TC}(\tilde{D}_n)_\#$. From Theorem 6.4, these chambers must be *faces* of either $\mathcal{P}D$ or $\mathcal{P}\tilde{D}$. Converting bracketings to tubings allows us to compute the face poset of the chamber using Theorem 6.6. The following is an example of this method. Note how there is not simply one type of polytope tiling each blown-up atypical complex, as was the case with the Coxeter complexes.

Example 6.15. By taking different bracketings in configurations $C_5(\mathbb{R}_o)$ associated to $\mathcal{C}(D_5)_\#$, we can produce the configuration space diagrams of different chambers of $\mathcal{C}(D_{4,1})_\#$, as in Figure 16. By converting bracketings to tubings using the bijection, each facet of the chamber corresponds to the appropriate reconnected complement.

The gluing rules for the compactified configuration spaces applies to these atypical models as well. The reflection action can change the ordering of standard and thick particles, and thus it encodes the manner in which polytopes of different types glue to tile the space.

Example 6.16. The illustration in Figure 17 of five chambers of $\mathcal{C}(D_{4,1})_\#$ shows how the configuration of three (standard) particles and 1 thick particle encodes gluing of faces among different types of chambers either across hyperplanes or antipodal maps. This is done by the flip action $\hat{\sigma}$ of Theorem 5.7. We see the gluing of a face of $\mathcal{P}D_4$ to a face of $\mathcal{P}X_4^a$ (a - b) and the corresponding labeled configuration spaces. Another face of this $\mathcal{P}X_4^a$ attaches to a face of $\mathcal{P}B_4$ (c - d) which glues to the face of another $\mathcal{P}B_4$ (e - f). This identification is across the hyperplane $x_i = 0$, where x_i is the label for the thick particle. Finally, this $\mathcal{P}B_4$ glues to another chamber of type $\mathcal{P}D_4$ (g - h) through an antipodal map.

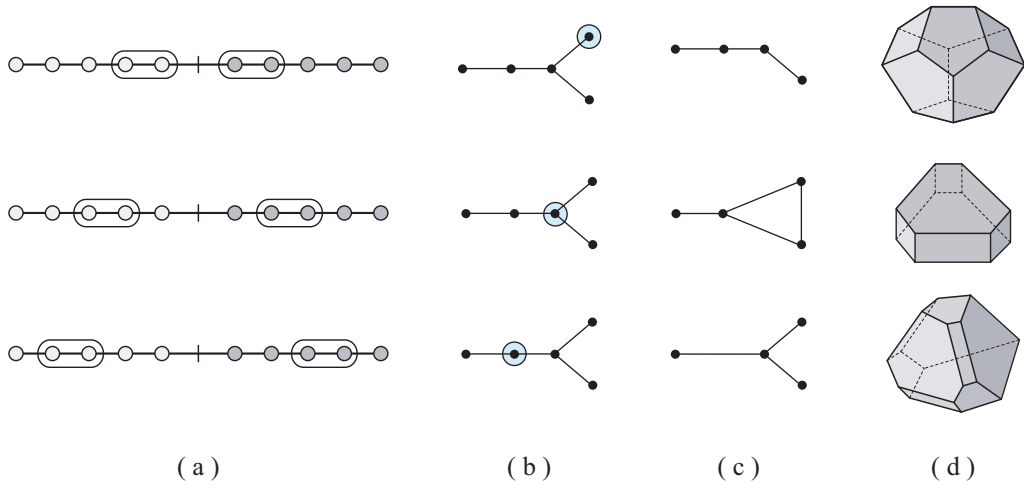


FIGURE 16. (a) Configuration diagram brackets, (b) associated tubing, (c) reconnected complements and (d) fundamental chambers.

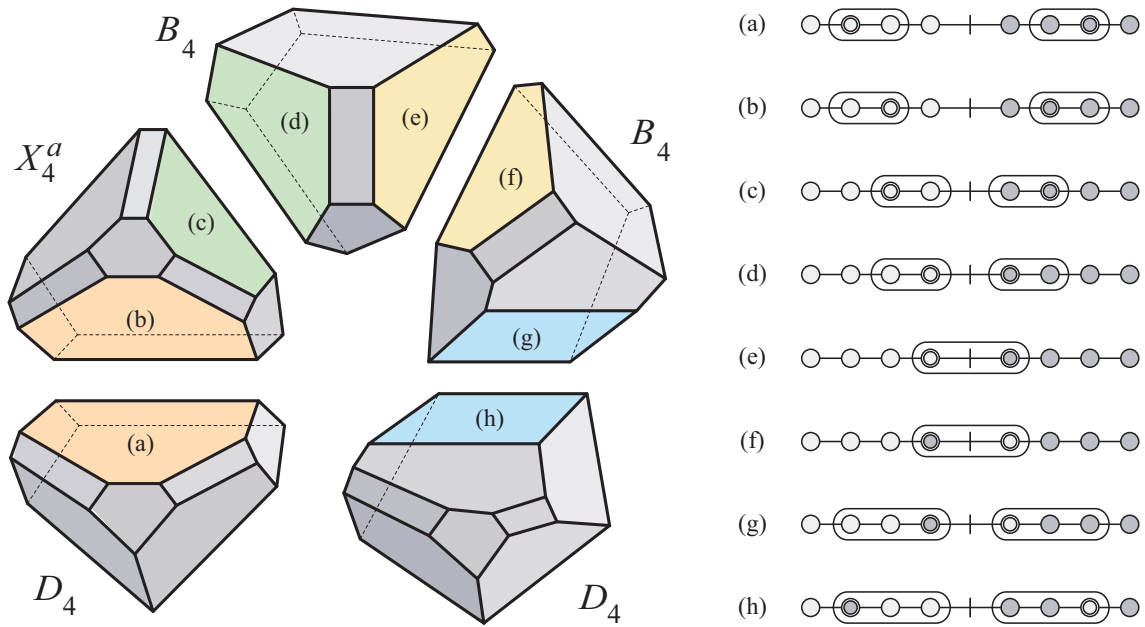


FIGURE 17. Five adjacent chambers in $\mathcal{C}(D_{4,1})_{\#}$.

CW	Subspace	Stabilizer	Enumeration	Configuration
$\mathcal{C}A_n$	$\mathcal{C}A_{k+1}$	A_{n-k-1}	$\binom{n+1}{n-k}$	
$\mathcal{C}B_n$	$\mathcal{C}B_{k+1}$	B_{n-k-1}	$\binom{n}{n-k-1}$	
	$\mathcal{C}B_{k+1}$	A_{n-k-1}	$2^{n-k-1} \binom{n}{n-k}$	
$\mathcal{C}D_n$	$\mathcal{C}B_{k+1}$	D_{n-k-1}	$\binom{n}{n-k-1}$	
	$\mathcal{C}D_{k+1,1}$	A_{n-k-1}	$2^{n-k-1} \binom{n}{n-k}$	
$\mathcal{C}D_{n,m}$	$\mathcal{C}B_{k+1}$	$D_{n-k-1,r}$	$\binom{m}{r} \binom{n-m}{n-k-r-1}$	
	$\mathcal{C}D_{k+1,m-r+1}$	A_{n-k-1}	$2^{n-k-1} \binom{n}{n-k}$	

TABLE 3. Minimal building sets of dimension k for spherical complexes.

CW	$\mathbb{T}\mathbb{C}\tilde{A}_n$	$\mathbb{T}\mathbb{C}\tilde{B}_n$			$\mathbb{T}\mathbb{C}\tilde{C}_n$	
Subspace	$\mathbb{T}\mathbb{C}\tilde{A}_{k+1}$	$\mathbb{T}\mathbb{C}\tilde{B}_{k+1,1}$	$\mathbb{T}\mathbb{C}\tilde{B}_{k+1}$	$\mathbb{T}\mathbb{C}\tilde{C}_{k+1}$	$\mathbb{T}\mathbb{C}\tilde{C}_{k+1}$	$\mathbb{T}\mathbb{C}\tilde{C}_{k+1}$
Stabilizer	A_{n-k}	A_{n-k-1}	B_{n-k}	D_{n-k}	A_{n-k-1}	B_{n-k}
Enumeration	$\binom{n+1}{n+1-k}$	$2^{n-k-1} \binom{n}{n-k}$	$\binom{n}{n-k}$	$\binom{n}{n-k}$	$2^{n-k-1} \binom{n}{n-k}$	$2 \binom{n}{n-k}$
Configuration						

CW	$\mathbb{T}\mathbb{C}\tilde{D}_n$	$\mathbb{T}\mathbb{C}\tilde{B}_{n,m}$			$\mathbb{T}\mathbb{C}\tilde{D}_{n,m}$	
Subspace	$\mathbb{T}\mathbb{C}\tilde{D}_{k+1,1}$	$\mathbb{T}\mathbb{C}\tilde{B}_{k,m-r+1}$	$\mathbb{T}\mathbb{C}\tilde{B}_{k+1,r}$	$\mathbb{T}\mathbb{C}\tilde{C}_{k+1}$	$\mathbb{T}\mathbb{C}\tilde{D}_{k+1,m-r+1}$	$\mathbb{T}\mathbb{C}\tilde{B}_{k+1,r}$
Stabilizer	A_{n-k-1}	A_{n-k-1}	B_{n-k-1}	$D_{n-k-1,r}$	A_{n-k-1}	$D_{n-k-1,r}$
Enumeration	$2^{n-k-1} \binom{n}{n-k}$	$2^{n-k-1} \binom{n}{n-k}$	$\binom{n-m}{n-k-r-1} \binom{m}{r}$	$\binom{n-m}{n-k-r-1} \binom{m}{r}$	$2^{n-k-1} \binom{n}{n-k}$	$2 \binom{n-m}{n-k-r-1} \binom{m}{r}$
Configuration						

TABLE 4. Minimal building sets of dimension k for Euclidean complexes.

REFERENCES

1. S. Axelrod, I. M. Singer, Chern-Simons perturbation theory II, *J. Diff. Geom.* **39** (1994) 173-213.
2. L. Billera, S. Holmes, K. Vogtmann, Geometry of the space of phylogenetic trees, *Adv. Appl. Math.* **27** (2001) 733-767.
3. R. Bott and C. Taubes, On the self-linking of knots, *J. Math. Phys.* **35** (1994) 5247-5287.
4. N. Bourbaki, *Lie Groups and Lie Algebras: Chapters 4-6*, Springer-Verlag, Berlin, 2002.
5. H. R. Brahana and A. M. Coble, Maps of twelve countries with five sides with a group of order 120 containing an icosahedral subgroup, *Amer. J. Math.* **48** (1926) 1-20.
6. M. Carr and S. L. Devadoss, Coxeter complexes and graph-associahedra, *Topology Appl.* **153** (2006) 2155-2168.
7. A. Cayley, On the partitions of a polygon, *Proc. Lond. Math. Soc.* **22** (1890) 237-262.
8. M. Davis, T. Januszkiewicz, R. Scott, Nonpositive curvature of blowups, *Selecta Math.* **4** (1998) 491 - 547.
9. C. De Concini and C. Procesi, Wonderful models of subspace arrangements, *Selecta Math.* **1** (1995) 459-494.
10. S. L. Devadoss, Tessellations of moduli spaces and the mosaic operad, *Contemp. Math.* **239** (1999) 91-114.
11. S. L. Devadoss, A space of cyclohedra, *Disc. Comp. Geom.* **29** (2003) 61-75.
12. S. L. Devadoss, Combinatorial equivalence of real moduli spaces, *Notices Amer. Math. Soc.* **51** (2004) 620-628.
13. P. Etingof, A. Henriques, J. Kamnitzer, E. Rains, The cohomology ring of the real locus of the moduli space of stable curves of genus 0 with marked points, preprint math.AT/0507514.
14. Z. Fiedorowicz, The symmetric bar construction, preprint.
15. K. Fukaya, Y-G Oh, H. Ohta, K. Ono, Lagrangian intersection Floer theory: anomaly and obstruction. *Kyoto. Dept. Math.* 00-17.
16. W. Fulton and R. MacPherson, A compactification of configuration spaces, *Ann. Math.* **139** (1994) 183-225.
17. A. Goncharov and Y. Manin, Multiple ζ -motives and moduli spaces $\overline{\mathcal{M}}_{0,n}$, *Compos. Math.* **140** (2004) 1-14.
18. R. Hartshorne, *Algebraic Geometry*, Springer-Verlag, New York, 1977.
19. M. M. Kapranov, The permutoassociahedron, MacLane's coherence theorem, and asymptotic zones for the KZ equation, *J. Pure Appl. Alg.* **85** (1993) 119-142.
20. M. Kontsevich and Y. Manin, Gromov-Witten classes, quantum cohomology, and enumerative geometry, *Comm. Math. Phys.* **164** (1994) 525-562.
21. D. Levy and L. Pachter. The neighbor-net algorithm, preprint math.CO/0702515.
22. M. Markl, S. Shnider, J. Stasheff, *Operads in Algebra, Topology and Physics*, Amer. Math. Soc., Rhode Island, 2002.
23. M. Markl, Homotopy Algebras are Homotopy Algebras, *Forum Math.* **16** (2004) 129-160.
24. D. Mumford, J. Fogarty, F. Kirwan, *Geometric Invariant Theory*, Springer-Verlag, New York, 1994.
25. T. Parker and J. Wolfson, Pseudo-holomorphic maps and bubble trees, *J. Geom. Anal.* **3** (1993) 63-98.
26. A. Postnikov, Permutohedra, associahedra, and beyond, preprint math.CO/0507163.
27. A. Postnikov, V. Reiner, L. Williams, Faces of generalized permutohedra, preprint math.CO/0609184.
28. E. Rains, The homology of real subspace arrangements, preprint math.AT/0610743.
29. R. Simion, A type-B associahedron. *Adv. Appl. Math.* **30** (2003) 2-25.
30. D. P. Sinha, Manifold-theoretic compactifications of configuration spaces, *Selecta Math.* **10** (2004) 391-428.
31. R. P. Stanley, *Enumerative Combinatorics: Volume 2*, Cambridge University Press, New York, 1999.
32. J. Stasheff, Homotopy associativity of H -spaces I, *Trans. Amer. Math. Soc.* **108** (1963) 275-292.
33. J. Stasheff (Appendix B coauthored with S. Shnider), *Contemp. Math.* **202** (1997) 53-81.

S. ARMSTRONG: WILLIAMS COLLEGE, WILLIAMSTOWN, MA 01267
E-mail address: `suzanne.m.armstrong@williams.edu`

M. CARR: UNIVERSITY OF MICHIGAN, ANN ARBOR, MI 48109
E-mail address: `mpcarr@umich.edu`

S. DEVADOSS: WILLIAMS COLLEGE, WILLIAMSTOWN, MA 01267
E-mail address: `satyan.devadoss@williams.edu`

E. ENGLER: WILLIAMS COLLEGE, WILLIAMSTOWN, MA 01267
E-mail address: `eric.h.engler@williams.edu`

A. LEININGER: MIT, CAMBRIDGE, MA 02139
E-mail address: `anandal@mit.edu`

M. MANAPAT: UNIVERSITY OF CALIFORNIA, BERKELEY, CA 94720
E-mail address: `manapat@ocf.berkeley.edu`